J Mater Sci: Mater Med (2010) 21:1913–1920
DOI 10.1007/s10856-010-4041-5

Interface processes between iron containing aluminosilicate systems and simulated body fluid enriched with protein

K. Magyari · O. Popescu · V. Simon

Received: 10 June 2009 / Accepted: 1 March 2010 / Published online: 12 March 2010

Abstract The behaviour of iron containing aluminosilicate samples in Kokubo's simulated body fluid (SBF) and in SBF enriched with bovine serum albumin (BSA) has been investigated. Crystalline samples of $(80–x)SiO_2{\cdot}20Al_2O_3{\cdot}xFe_2O_3$ system, with x = 5, 10 or 15 mol%, obtained by sol–gel method and heat treated at 1200°C in air for 24 h. Data on electrical conductivity, calcium, phosphorous and potassium concentrations in simulated body fluids after samples soaking in static regime at 37°C, for several periods up to 14 days, were used to estimate the dynamics of these cations on the interface of aluminosilicate samples with SBF, and with SBF containing BSA. The UV-visible and fluorescence spectra recorded from the simulated body fluids after immersion of the investigated aluminosilicate samples evidence changes function on immersion time and Fe_2O_3 content.

1 Introduction

Microparticles of silicate systems containing iron oxide are investigated for their potential application in hyperthermia treatments [1–4]. Localized magnetic hyperthermia shows promise as a treatment modality for tumor eradication [5]. The most common approach for difficult access location in the body is the use of injectable thermoseeds which can be remotely heated [6]. Magnetic nanoparticles are also applied in improving the quality of magnetic resonance imaging, site-specific drug delivery and the manipulation of cell membranes [7]. Superparmagnetic nanoparticles bearing negative surface charge behave as anions and show a high affinity for the cell membrane and, as a consequence, are captured by cells with very high efficiency. Anionic maghemite nanoparticles strongly and nonspecifically interact with the plasma membrane, due to their negative charges, and exhibit a high level of cell internalization. The adsorption step preceding the internalization step governs the overall cell uptake [7, 8].

Regardless of their dimensions, the behavior of all biomaterials in the human body is strongly influenced by the properties of their surface, which is first coming in contact with the body fluid and the proteins contained therein. The interaction of material surfaces with biological matter is of great importance, because the manner in which the surface interacts with biomolecules contributes strongly to the success or failure of a biomaterial. Surface energy is a fundamental material property that affects cell interactions. Although direct cell-material interaction is not excluded, the indirect interaction is probably more important as surface energy first dictates protein adsorption, which subsequently influences cell response. Biocompatibility is mainly determined by the manner in which the biomaterial surfaces interact with blood constituents and implicitly with proteins [9, 10]. SBF proposed by Kokubo et al. [11] is the most frequently used solution simulating the body fluid for in vitro tests, because it contains inorganic ions in concentrations very close to those of human blood plasma. In the circulatory system, the most abundant protein, accounting for 60% of the total serum protein, is serum albumin. The albumin released into circulation

K. Magyari · V. Simon (✉)
Faculty of Physics and Institute for Interdisciplinary Experimental Research, Babes-Bolyai University, Cluj-Napoca, Romania
e-mail: viosimon@phys.ubbcluj.ro

O. Popescu
Faculty of Biology and Geology and Institute for Interdisciplinary Experimental Research, Babes-Bolyai University, Cluj-Napoca, Romania

possesses a half-life of 19 days [12]. The main function of serum albumin is to transport metabolites in blood [12, 13]. They can bind a wide variety of ligands, e.g., fatty acid, bilirubin and drugs [13]. The bovine serum albumin is commonly used in several studies to simulate human albumin, due to the structural homology of the two proteins [14]. Both human and bovine serum albumin are large globular proteins about 66 kDa [15, 16].

The purpose of this work is to study the interaction of iron containing aluminosilicate systems with the protein bovine serum albumin (BSA) in simulated body fluid (SBF) solution. The interaction between iron containing aluminosilicate samples and BSA-enriched SBF was studied by electrochemical measurements, inductively coupled plasma mass spectrometry, UV absorption and fluorescence spectroscopy.

2 Experimental

Samples of $(80–x)SiO_2{\cdot}20Al_2O_3{\cdot}xFe_2O_3$ system, with $x = 5$, 10 or 15 mol%, were prepared by sol–gel method using as starting reagents $Si(OH)_4$, $Al(NO_3)_3{\cdot}9H_2O$, $Fe(NO_3)_3{\cdot}9H_2O$. Silicic acid was dissolved in distilled water and mixed at room temperature about 30 min. After addition of $Al(NO_3)_3{\cdot}9H_2O$ water solution the mixture was stirred for 30 min at 90 °C, and the $Fe(NO_3)_3{\cdot}9H_2O$ water solution was then added. As the mixture appeared like a gel, it was filtered and dried in an electric oven at 110°C for 20 h. The pH of the prepared samples was 8.5. The dried samples were treated at 1200°C in air for 24 h and undercooled at room temperature. The surface area of the samples was estimated in the order of tens of m^2/g. X-ray diffraction analysis of iron containing aluminosilicate samples heat treated at 1200°C revealed the development of hematite (α-Fe_2O_3), maghemite (γ-Fe_2O_3), mullite ($Al_6Si_2O_{13}$) and crystoballite (SiO_2) crystalline phases with crystals of nanometric size [17].

In order to check the bioactivity of the samples with different Fe_2O_3 contents, fine powdered samples of the investigated compositions were immersed in SBF, and in SBF containing BSA, in conical polypropylene flask. The flasks were kept under static conditions in an incubator at the constant temperature of 37°C for 3, 7 and 14 days. The SBF was prepared according to Kokubo's protocol [11] by dissolving in deionised water NaCl, $NaHCO_3$, KCl, $K_2HPO_4{\cdot}3H_2O$, $MgCl_2{\cdot}6H_2O$, $CaCl_2$, HCl (1 M), Na_2SO_4 and $NH_2C(CH_2OH)_3$. The solution was buffered at pH 7.38 at room temperature. The inorganic ion concentrations in the SBF solution are almost the same as those in human blood plasma. However beside the inorganic components there are many organic compounds in human blood plasma, which are not included in Kukobo's SBF solution. For this reason a solution containing bovine serum albumin was prepared by dissolving 1 mg/ml BSA in SBF.

After each immersion stage the concentration of Ca, P and K ions in the immersion solutions was measured using an inductively coupled plasma mass spectrometer ICP-TOF-MS model Optimass 9500. Conductivity of SBF, and SBF containing BSA solutions before and after immersion of samples for different periods was measured at room temperature with Consort C833 digital multimeter. An average of three measurements was taken in all cases. The UV spectra were recorded using a Jasco UV-Visible spectrometer V-530 in the spectral range from 240 to 400 nm. Measurements of fluorescence were performed on Jasco spectrofluorimeter FP-6300. The excitation wavelength was 295 nm and fluorescence spectra were recorded from 300 to 450 nm. In all measurements the analysed solutions were extracted from the flaks containing the soaked samples.

3 Results and discussion

As biomaterials are immersed in a liquid phase containing a protein, a reorganization of the protein is expected on biomaterial surface [18]. The interface processes are influenced by the release of cations from biomaterial into biological medium and the further self-assembly of these cations on biomaterial surface. Aluminosilicate systems are characterized by high corrosion stability [19], but in biological fluids they can become bioactive due to their surface reactivity, at least temporary [20, 21]. The variation of Ca^{2+} concentration in SBF, and SBF containing BSA solutions wherein the investigated alumionosilicate powders were tested is shown in Fig. 1 as function of soaking time. For all samples, after 3 days of immersion, the Ca^{2+} concentration in the simulated body fluids was diminished. This indicates that part of the calcium ions from SBF are self-assembled on the samples surface. It also has to be noticed that the calcium ions concentration in the BSA-enriched SBF was slightly lower for all samples after 3 days immersion (Fig. 1a), denoting that in the presence of the protein a higher number of calcium ions are directed and attached onto samples surface. This result is clearly a consequence of BSA binding on samples surface. The data plotted in Fig. 1 also indicate that the highest values of Ca^{2+} concentration in solutions are obtained for the sample with 15 mol.% Fe_2O_3 in SBF, suggesting that the self-assembly on sample surface of structural units implying calcium is initially restricted by increasing iron content.

At the same time the phosphorus concentration pronouncedly decreased in the simulated body fluids extracted after 3 days (Fig. 2). After immersion of samples with similar composition, the phosphorous concentration in SBF

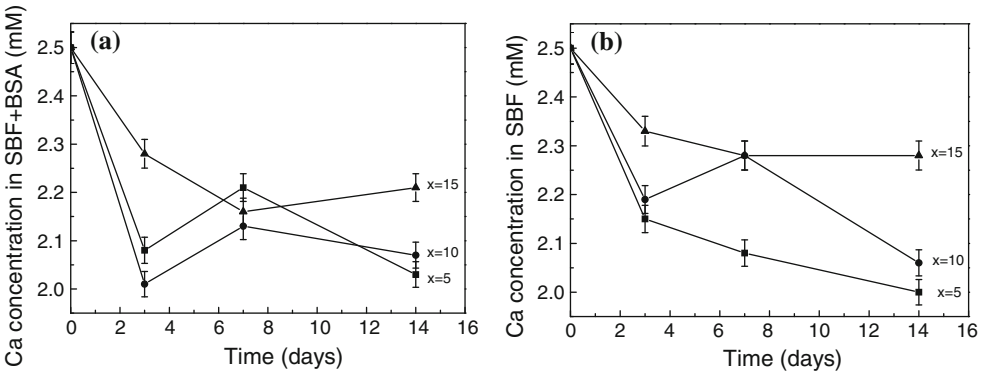

Fig. 1 Time dependence of calcium concentration in SBF with BSA (**a**) and SBF solution (**b**)

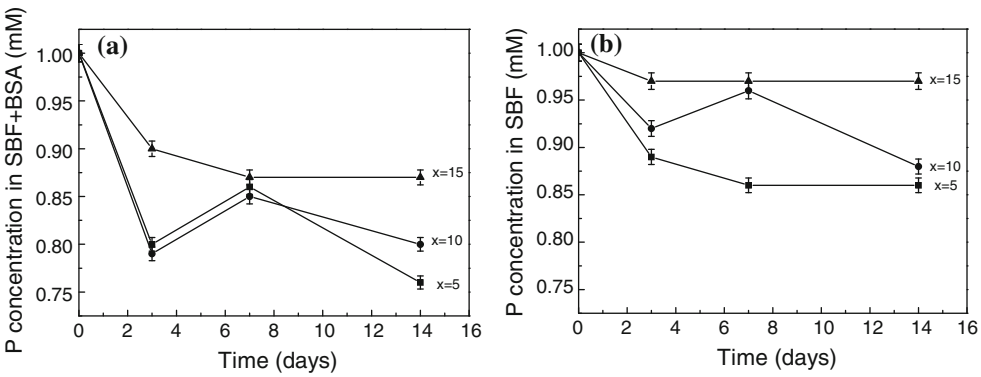

Fig. 2 Time dependence of phosphorous concentration in SBF with BSA (**a**) and SBF solution (**b**)

and BSA-enriched SBF varies according to the different soaking times. Similar to the results obtained for Ca^{2+} concentration, in the protein-enriched SBF solution (Fig. 2a) the concentration of phosphorus ions decreases under the values measured in SBF solutions without BSA (Fig. 2b). This points out that BSA contributes to the extraction and deposition on the surface of aluminosilicate samples of more phosphorus from the biological media [22].

The above results show that the samples acquire from the soaking environments both calcium and phosphorus ions, which could form calcium–phosphate structure due to the aggregation between Ca^{2+} and PO_4^{3-} ions [20]. In water solution the Si–OH groups formed on the surface provide nucleation sites for apatite formation [23]. The increase of calcium and phosphorus concentration in the studied fluids after 7 days, in the case of samples with lower iron content, shows that the initially formed calcium and phosphorus rich layer on the aluminosilicate particles is not stable. After 14 days this layer is more consistent and much dependent upon iron content. In this approach, according to our data regarding Ca^{2+} and P^{5+} concentration in simulated body fluids, the thickness of self-assembled hydroxyapatite type layer is expected to be diminished by increase of Fe_2O_3 content in the aluminosilicate matrix.

The K^+ concentration as function of soaking time (Fig. 3) proves the property of albumin to bind potassium ions and attach on samples in the first immersion stage.

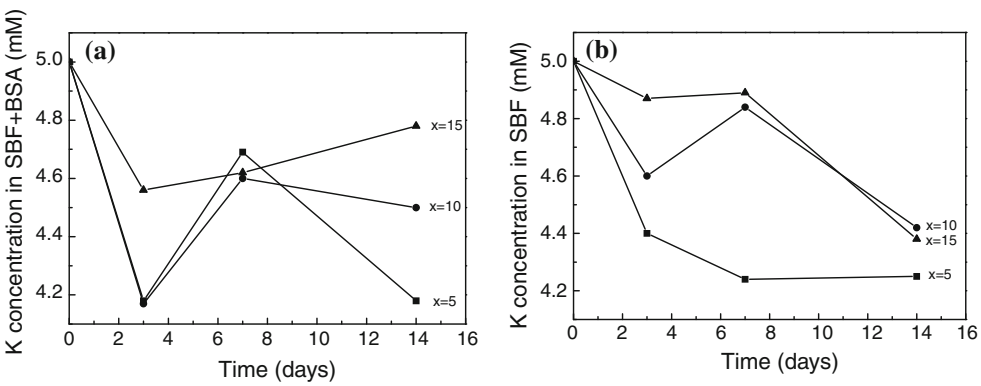

Fig. 3 Time dependence of potassium concentration in SBF with BSA (**a**) and SBF solution (**b**)

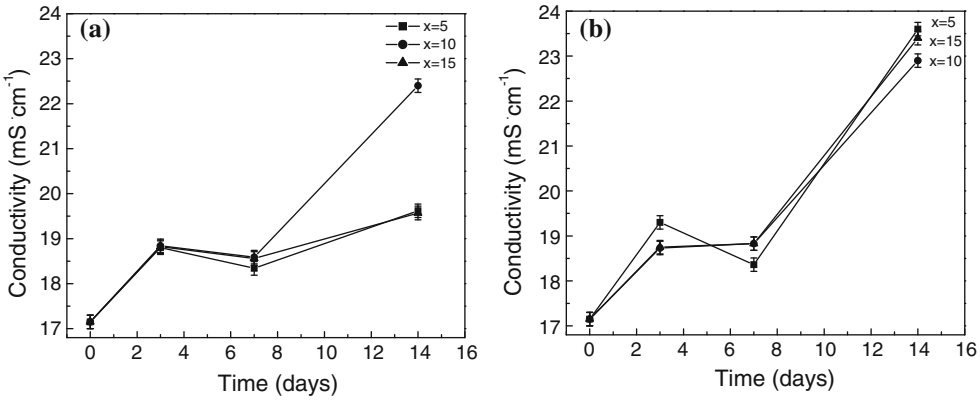

Fig. 4 Time dependence of conductivity of SBF with BSA (**a**) and SBF solution (**b**)

A release of K^+ ions is observed for all samples (Fig. 3a) between the third and the seventh soaking days. After 3 days one observes for the samples with $x = 5$ and 10 mol.% Fe_2O_3 that some of calcium and phosphorus ions (Figs. 1a and 2a) go back into BSA-SBF solution. Ca^{2+} and P^{5+} concentration further decreases in case of $x = 15$ mol.% Fe_2O_3 sample. After 2 weeks the changes are weaker, but generally they are still noticed. It is reported [24, 25] that in SBF solutions calcium phosphates of hydroxyapatite type are formed and transformed by dissolution-reprecipitation.

Figure 4 illustrates the electrical conductivity of the simulated body fluids as function of the soaking time. All cations existing in solutions contribute to their conductivity. Both in SBF and protein-enriched SBF the conductivity of the solutions increases after 7 days soaking time, more quickly in the solution without protein. Considering the soaking time dependence for the concentration of calcium, phosphorus and potassium ions (Figs. 1, 2, and 3), the time dependence of the conductivity could be explained only on the account of other cations arrived in solution from therein soaked samples, namely the iron ions. One can remark once more that the dynamics of the cations at the interface between samples and immersion solution is influenced by the addition to SBF of the protein which early adheres onto samples surface.

Since the measurements of Ca, P and K concentrations started after three soaking days, in order to search into the interactions of the protein with the SBF solution and with the samples surface prior to this moment, we have investigated by UV-Vis and fluorescence spectroscopy the BSA-enriched SBF solutions during 72 h after samples immersion.

Protein adsorption on various materials has been widely studied and it has been found that electrostatic, hydrophobic and specific chemical interactions play an important role between protein and the adsorbent materials [26, 27]. The sol–gel silicate materials have high surface area and porosity which facilitates protein-silica interaction but may lead to protein denaturation [28, 29].

Variation of BSA concentration in SBF solution after different soaking time of the investigated samples was determined using UV-visible spectroscopy. A calibration curve was obtained using known concentration of BSA at the absorbance maximum of 280 nm. The ε absorption coefficient was determined to be 0.6725 mg ml^{-1} cm^{-1}. The BSA concentration in SBF solutions with samples of different iron oxide contents was determined using the calibration curve. Two absorption bands arising from BSA are recorded in the UV-Vis spectra (Fig. 5) around 220 and 278 nm. In the spectral range explored, the bands around 278 nm show an intensity decrease in the first hours even

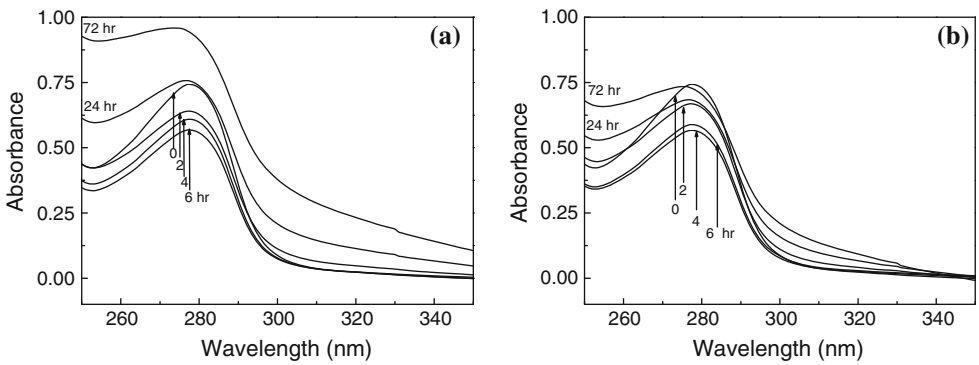

Fig. 5 Time dependent changes in UV-Vis spectrum of BSA in SBF (**a**) and of BSA in SBF with $65SiO_2{\cdot}20Al_2O_3{\cdot}15Fe_2O_3$ sample (**b**)

for BSA in SBF solution (Fig. 5a), that suggests an interaction of BSA with the cations from SBF. The increase of the band intensity in the spectra recorded after 24 and 72 h appears irregular. In addition, these absorption peaks have a slight blue shift from 278 to 275 nm. Similar effects are observed in the first 6 h for the solution with aluminosilicate sample (Fig. 5b), but intensities after 24 and 72 h are less increased than in the solution without sample.

The immersion of iron containing aluminosilicate samples in BSA-enriched SBF lead very early, already in the first 6 h, to changes of BSA concentration in SBF solution (Table 1). The decrease of BSA concentration in SBF solutions points out that the protein adheres onto samples surface. We appreciate that BSA binding to samples surface is accomplished in the first hours of immersion. The protein binding could be achieved by surface complexation of the positively charged sites of BSA (NH_3^+) with the silicon negatively charged sites (SiO^-) and that is likely to be an important factor in the dissolution process [30]. It was assumed that a hydrated silica formed on the surfaces of silicate materials in the body plays an important role in forming a surface apatite type layer and it was experimentally shown that a pure hydrated silica gel can induce apatite formation on its surface in a simulated body fluid [31]. For silicate bioactive glasses it was considered that in protein-free solutions the formation of a hydroxyapatite layer hinders the release of all silicon, since it acts as a protective layer, but when bioactive glasses are immersed in protein containing serum solutions, a porous and amorphous layer of silica, proteins and calcium phosphates is formed, which does not protect the glass from further corrosion [32]. Indeed, it was demonstrated that the in vivo bioactivity of these glasses is accurately reproduced by apatite-forming ability in SBF [33].

BSA is made up of three homologous domains (I, II, III), which are divided into nine loops (L1–L9) by 17 disulfide bonds. The loops in each domain are made up of a sequence of large–small–large loops forming a triplet. Each domain in turn is the product of two sub-domains [34]. BSA has two tryptophan residues, Trp-134 and Trp-212, embedded in the first sub-domain IB and sub-domain IIA, respectively. Trp-212 is located within a hydrophobic binding pocket of the protein and Trp-134 is located on the surface of the albumin molecule [35]. A valuable feature of intrinsic fluorescence of BSA is the high sensitivity of tryptophan to its local environment. Changes in emission spectra of tryptophan provide information on its interaction with the ligand [36]. Both bovine serum albumine and human serum albumin excited at 290 nm emit fluorescence attributable mainly to tryptophan residues [37, 38]. Fluorescence spectroscopy is a very sensitive experimental technique to changes in the local environment of the fluorophore [39]. The fluorescence intensity can be decreased by several molecular interactions like excited-state reactions, molecular rearrangements, energy transfer, ground state complex formation and collisional quenching [40]. Such decrease in intensity is called fluorescence quenching. Fluorescence quenching has been widely used as a powerful tool to reveal the accessibility of fluorophores in the protein matrix to quenchers and to investigate changes in the tertiary structure induced by the protein interaction with ionic surfactants. When a fluorophore absorbs a photon, an energetically excited state is formed, depending upon the nature of the fluorophore and its surroundings, which finally will loss the energy and return to the ground state. The ratio of photons absorbed to photons emitted through fluorescence is defined as fluorescence quantum yield. The quantum yield gives the probability of the excited state to be deactivated by fluorescence rather than by another, non-radiative mechanism. The changes determined by these interactions, in the position or orientation of the BSA tryptophan residues, affect their exposure to solvent, leading to alterations on the fluorescence quantum yield [12]. The positions of the two fluorescent tryptophan radicals of BSA are different, one of them is near the surface and the other is deeper and therefore is less accessible to surfactants. BSA has strong fluorescence at $\lambda_{ex}/\lambda_{em} = 295/343$ nm [40].

The fluorescence quenching spectra in our study were obtained at excitation and emission wavelengths of 295 and 300–450 nm, respectively, and they were recorded at different periods, up to 7 days. Before going into discussion of surfactant–protein interaction, we will present the fluorescence results showing how the SBF solution is affected by BSA protein. As can be observed for BSA-enriched SBF solution without soaked sample (Fig. 6) excepting the results obtained after 4 and 6 h, the fluorescence intensity of BSA continuously decreases and a slight blue shift is clearly recorded after 7 days, which indicates changes related to the chromophore of BSA. The slight blue shift of the emission maximum suggests a less polar, or more hydrophobic, environment of tryptophan residues [40]. As compared to the fluorescence emission spectra of BSA in SBF wherein samples of different iron contents are soaked,

Table 1 Dependence of BSA concentration in SBF solution (initially 1 mg/ml) on the soaking time of $(80–x)SiO_2{\cdot}20Al_2O_3{\cdot}xFe_2O_3$ samples

x (mol %)	Immersion time (hours)			
	0	2	4	6
	Concentration (mg/ml) (±0.03)			
5	1	0.99	0.91	0.90
10		1	0.91	0.91
15		0.98	0.87	0.83

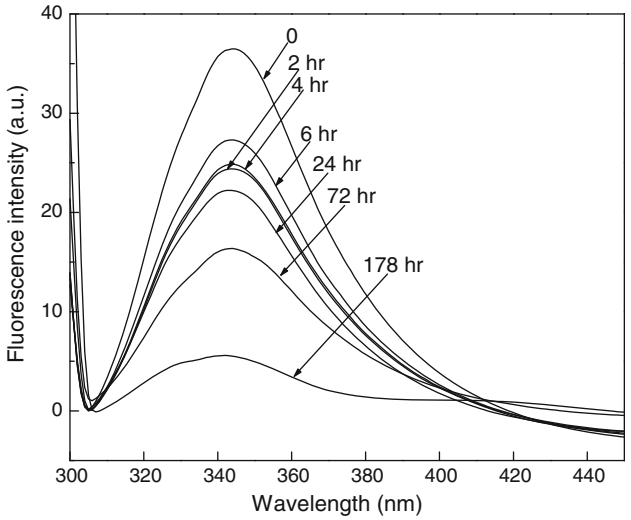

Fig. 6 Time dependent changes in fluorescence emission spectra of BSA in SBF

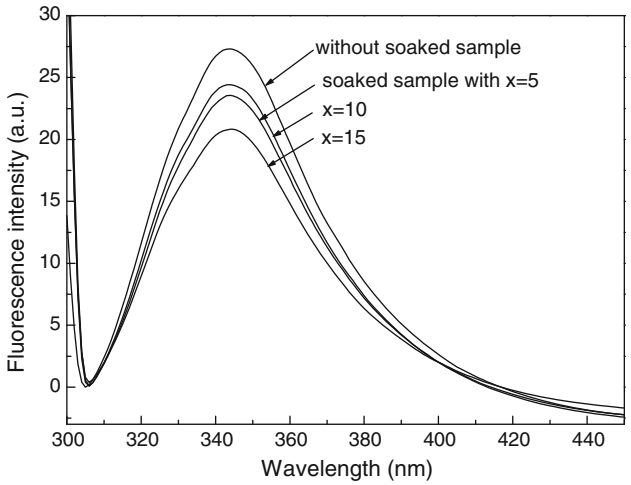

Fig. 7 Fluorescence emission spectra of BSA in SBF as a function of Fe_2O_3 concentration after 6 h incubation of $(80–x)SiO_2{\cdot}20Al_2O_3{\cdot}xFe_2O_3$ samples

one observes the decrease of fluorescence intensities with increasing iron concentration (Fig. 7).

Two quenching processes are known, static and dynamic quenching. Both of them require molecular contact between the fluorophore and the quencher. Static quenching refers to formation of a nonfluorescent fluorophore–quencher complex. Dynamic quenching refers to the quencher diffusion to the fluorophore during the lifetime of the excited state and upon contact the fluorophore returns to the ground state, without emission of a photon [41]. Both static and dynamic processes are described by the Stern–Volmer equation using the ratio between the fluorescence intensities in the absence and presence of the quencher, expressed as the area under the corresponding emission peaks [12].

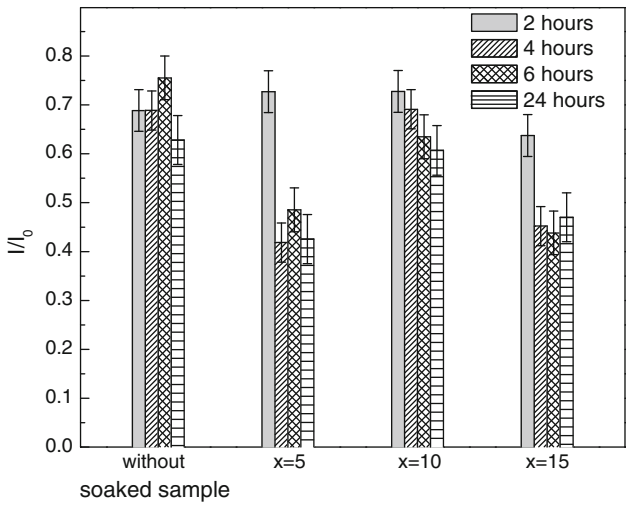

Fig. 8 Fluorescence quenching yields of BSA enriched SBF during 24 h without and with $(80–x)SiO_2{\cdot}20Al_2O_3{\cdot}xFe_2O_3$soaked samples

The fluorescence quenching yields obtained for the investigated samples are shown in Fig. 8. One remarks the BSA florescence quenching in SBF without soaked samples, due to the protein interaction with the ions from SBF, and at the same time a relative increase tendency after 6 h. The soaking of iron containing aluminosilicate samples contributes to protein fluorescence quenching, that is also influenced by Fe_2O_3 content. These findings highlight not only the fluorescence quenching, but also the fact that during the 24 h an increase in fluorescence is also possible.

The analysis carried out by Ross and Subramanian [42] on thermodynamic parameters characterizing the self-association and ligand binding of proteins has shown the impossibility to account for the stability of association complexes of proteins on the basis of hydrophobic interactions alone. They proposed a two steps model for protein association: (*i*) mutual penetration of hydration layers causing disordering of the solvent and further (*ii*) short-range interactions. Considering the thermochemical behavior of small molecule interactions, they concluded that the strengthening of hydrogen bonds inside macromolecules, and van der Waals interactions introduced as a consequence of the hydrophobic effect are the most important factors contributing to the stability of protein association complexes. The non-covalent interactions implied in the forces responsible for ligand-receptor stability and ultimately for stabilizing a native protein are four and can be classified based on the governing forces into three groups: (*a*) electrostatic; (*b*) hydrogen bonding; and (*c*) apolar, which includes van der Waals and hydrophobic bonds interactions [43]. When these molecules bind to a globular protein, the intramolecular forces responsible for maintaining the secondary and tertiary structures can be altered, resulting in a conformational change of the protein [44]. For low concentration of

surfactants the binding is to specific high energy sites on the protein and the interactions are mainly electrostatic, but hydrophobic contributions are not excluded. It is assumed that during the immersion time the surfactant acts differently, and can have anionic, cationic or zwitterionic character. The anionic surfactant leads to fluorescence quenching, while the cationic and zwitterionic surfactants induce the enhancement of fluorescence observed for BSA [12]. The irregular increase of fluorescence intensity apparently unexpected in the spectra recorded after 24 and 72 h (Fig. 5) can be explained by the prevalent cationic or zwitterionic character achieved by surfactants.

The qualitative investigation based on fluorescence quenching yields obtained for increasing exposure time of the tryptophan residues in the BSA protein in SBF, in the absence and the presence of iron containing aluminosilicate samples, suggests that an equilibrium of the native protein, intermediate species of surfactant-bound protein and partially denatured protein is very probably realized by interactions with surface active agents of both anionic, and cationic or zwitterionic character.

4 Conclusions

Protein binding aluminosilicate samples containing iron oxide were obtained by immersion in simulated body fluid enriched with BSA. The protein binding onto surface is achieved in the first 6 h after incubation. The values of calcium and phosphorus concentration in simulated body fluids after immersion of samples suggest that the self-assembly on sample surface of calcium phosphate type units is restricted by increasing iron content. The dependence of electrical conductivity of simulated body fluid on sample incubation time could be also considered on the account of iron ions released from aluminosilicate samples. The offtake of calcium and phosphorus ions from SBF on sample surface is enhanced by protein binding. The slight blue shift of the fluorescence emission maximum of BSA in SBF indicates that in the presence of iron containing aluminosilicate samples the environment of tryptophan residues becomes less polar due to the binding by albumin of the cations from SBF soaking solution. The time dependence of fluorescence quenching yield qualitatively points to both electrostatic and apolar interactions.

References

1. Bretcanu O, Spriano S, Verné E, Cöisson M, Tiberto P, Allia P. The influence of crystallised Fe_3O_4 on the magnetic properties of coprecipitation-derived ferrimagnetic glass-ceramics. Acta Biomater. 2005;1:421–9.
2. Nakamura H, Kishi T, Ohgaki T, Muro Y, Yasumori A. Magnetic properties of phase separated glasses and glass ceramics in Co_3O_4–TiO_2–SiO_2 system. J Phys Conf Ser. 2008;106:012009.
3. Eniu D, Cacaina D, Coldea M, Valeanu M, Simon S. Structural and magnetic properties of CaO–P_2O_5–SiO_2–Fe_2O_3 glass-ceramics for hyperthermia. J Magn Magn Mater. 2005;293:310–3.
4. Simon V, Mocuta H, Eniu D, Trandafir D, Simon S. Structural investigation of composite biomaterials for hyperthermia. Eur Cells Mater. 2007;13S3:6.
5. Gross KA, Jackson R, Cashion JD. Rodriguez-Lorenzo LM. Eur Cells & Mater. 2002;3S(2):114–7.
6. Fuwa N, Nomoto Y, Shouji K, Kodaira T, Kamata M, Ito Y. Therapeutic effects of simultaneous intraluminal irradiation and intraluminal hyperthermia on oesophageal carcinoma. Brit J Radiol. 2001;74:709–14.
7. Berry CC, Curtis ASG. Functionalisation of magnetic nanoparticles for applications in biomedicine. J Phys D Appl Phys. 2003;36:R198–206.
8. Wilhelm C, Billotey C, Roger J, Pons JN, Bacri JC, Gazeau F. Intracellular uptake of anionic superparamagnetic nanoparticles as a function of their surface coating. Biomaterials. 2003;24:1001–11.
9. Cheung AK. Biocompatibility of hemodialysis membranes. J Am Soc Nephrol. 1990;1:150–61.
10. Cavalu S, Simon V, Bănică F, Deleanu C. Fibrinogen adsorption onto bioglass aluminosilicates. Rom J Biophys. 2007;17:237–45.
11. Kokubo T, Kushitani H, Sakka S, Kitsugi T, Yamamuro T. Solutions able to reproduce in vivo surface-structure changes in bioactive glass-ceramic A-W3. J Biomed Mater Res. 1990;24:721–34.
12. Gelamo EL, Tabak M. Spectroscopic studies on the interaction of bovine (BSA) and human (HSA) serum albumins with ionic surfactants. Spectrochim Acta A. 2000;56:2255–71.
13. De S, Girigoswami A, Das S. Fluorescence probing of albumin-surfactant interaction. J Colloid Interf Sci. 2005;252:562–73.
14. He XM, Carter DC. Atomic structure and chemistry of human serum albumin. Nature. 1992;358:209–15.
15. Dockal M, Carter DC, Ruker F. Conformational transitions of the three recombinant domains of human serum albumin depending on pH. J Biol Chem. 2000;275:3042–50.
16. Hains PG, Sung K-L, Tseng A, Broady KW. Functional characteristics of a phospholipase A2 inhibitor from Notechis ater serum. J Biol Chem. 2000;275:983–91.
17. Tamasan M, Radu T, Simon S, Barbur I, Mocuta H, Simon V. Thermal analysis of sol-gel aluminosilicate systems. J Optoelectr Adv Mater. 2008;10:948–50.
18. Amaral M, Lopes MA, Santos JD, Silva RF. Wettability and surface charge of Si_3N_4-bioglass composites in contact with simulated physiological liquids. Biomaterials. 2002;23:4123–9.
19. Erbe EM, Day DE. Properties of Sm_2O_3–Al_2O_3–SiO_2 glasses for in vivo applications. J Am Ceram Soc. 1990;73:2708–13.
20. Tilocca A, Cormack AN, De Leeuw NH. The structure of bioactive silicate glasses: new insight from molecular dynamics simulations. Chem Mater. 2007;19:95–103.
21. Tilocca A, Cormack AN. Exploring the surface of bioactive glasses: water adsorption and reactivity. J Phys Chem C. 2008;112:11936–45.
22. Magyari K, Tănăselia C, Simon V. Dynamics of calcium, phosphorus and sodium ions at the interface of sol-gel hydroxyapatite with simulated body fluid. J Optoelectron Adv Mater. 2008;10:951–3.
23. Ryu HS, Lee J-K, Seo J-H, Kim H, Homg KS, Kim DJ, et al. Novel bioactive and biodegradable glass ceramics with high mechanical strength in the CaO–SiO_2–B_2O_3 system. J Biomed Mater Res A. 2004;68:79–89.

24. Granqvist B, Helminen A, Vehviläinen M, Ääritalo V, Seppälä J, Lindén M. Biodegradable and bioactive hybrid organic-inorganic PEG-siloxane fibers. Preparation and characterization. Colloid Polym Sci. 2004;282:495–501.
25. Cacaina D, Ylänen H, Hupa M, Simon S. Study of yttrium containing bioactive glasses behaviour in simulated body fluid. J Mater Sci Mater Med. 2006;17:709–16.
26. Patil S, Sandberg A, Heckert E, Self W, Seal S. Protein adsorption and cellular uptake of cerium oxide nanoparticles as a function of zeta potential. Biomaterials. 2007;28:4600–7.
27. Mansur HS, Oréfice RL, Vasconelos WL, Lobato ZP, Machado LJC. Biomaterial with chemically engineered surface for protein immobilization. J Mater Sci Mater Med. 2005;16:333–40.
28. Flora K, Brennan J. Effect of matrix aging on the behavior of human serum albumin entrapped in a tetraethyl orthosilicate-derived glass. Chem Mater. 2001;13:4170–9.
29. Simon V, Cavalu S, Simon S, Mocuta H, Vanea E, Prinz M, et al. Surface functionalisation of sol-gel derived aluminosilicates in simulated body fluids. Solid State Ionics. 2009;180:764–9.
30. Kawano M, Hashizume H, Hwang J. The effect of BSA on the dissolution rates of amorphous silica in solution at different pH. Geochim Cosmochim Acta. 2008;72S1:A455.
31. Li P, Ohtsuki C, Kokubo T, Nakanishi K, Soga N, Nakamura T, et al. Apatite formation induced by silica gel in a simulated body fluid. J Am Ceram Soc. 2005;75:2094–7.
32. Radin S, Ducheyne P, Falaize S, Hammond A. In vitro transformation of bioactive glass granules into Ca–P shells. J Biomed Mater Res. 2000;49:264–72.
33. Fujibayashi S, Neo M, Kim HM, Kokubo T, Nakamura T. A comparative study between in vivo bone ingrowth and in vitro apatite formation on Na_2O–CaO–SiO_2 glasses. Biomaterials. 2003;24:1349–56.
34. Papadopoulou A, Green RJ, Frazier RA. Interaction of flavonoids with bovine serum albumin: a fluorescence quenching study. J Agr Food Chem. 2005;53:158–63.
35. Peters T Jr. Serum albumin. Adv Protein Chem. 1985;37:161–245.
36. Sulkowska A. Interaction of drugs with bovine and human serum albumin. J Mol Struct. 2002;614:227–32.
37. Sun C, Yang J, Wu X, Huang X, Wang F, Liu S. Unfolding and refolding of bovine serum albumin induced by cetylpyridinium bromide. Biophys J. 2005;88:3518–24.
38. Hu YJ, Liu Y, Pi ZB, Qu SS. Interaction of cromolyn sodium with human serum albumin: a fluorescence quenching study. Bioorg Med Chem. 2005;13:6609–14.
39. Ladokhin AS. Fluorescence spectroscopy in peptide and protein analysis. In: Meyers RA, editor. Encyclopedia of analytical chemistry. Chichester: JohnWiley; 2000. p. 5762–79.
40. Hu YJ, Liu Y, Zhang LX, Zhao RM, Qu SS. Studies of interaction between colchicine and bovine serum albumin by fluorescence quenching method. J Mol Struct. 2005;750:174–8.
41. Lakowicz JR. Principles of fluorescence spectroscopy. New York: Plenum Press; 1983.
42. Ross PD, Subramanian S. Thermodynamics of protein association reactions: forces contributing to stability. Biochemistry. 1981;20:3096–102.
43. Klotz IM. Ligand-receptor complexes: origin and development of the concept. J Biol Chem. 2004;279:1–12.
44. Parker W, Song PS. Protein structures in SDS micelle-protein complexes. Biophys J. 1992;61:1435–9.